Electronic Supplementary Material (ESI) for Journal of Materials Chemistry A.

Simultaneous optimization of CoIr alloy nanoparticle and 2D graphitic-N doped carbon support in CoIr@CN by Ir doping for enhanced oxygen and hydrogen evolution reaction

Weibin Chen [a], Yuxin Xie [a], Xuehui Gao [b], Lei Li [a]*, Zhan Lin [a]*

[a] *Guangdong Provincial Key Laboratory of Plant Resources Biorefinery, School of Chemical Engineering and Light Industry, Guangdong University of Technology, Guangzhou 510006, China*

[b] *Department of Chemistry, Key Laboratory of the Ministry of Education for Advanced Catalysis Materials, Zhejiang Normal University, Jinhua 321004, China*

*Corresponding authors. *E-mail address*: li.lei@gdut.edu.cn, zhanlin@gdut.edu.cn

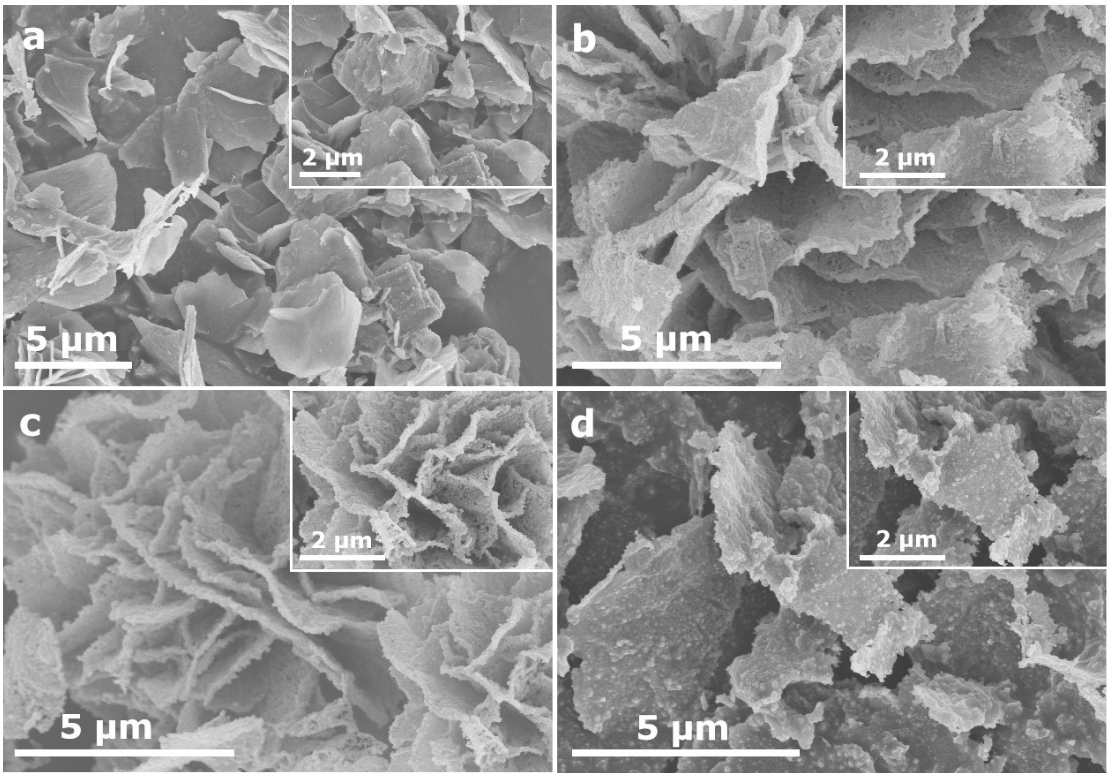

Figure S1. SEM images of (a) Co@CN, (b) CoIr@CN-0.15, (c) CoIr@CN-0.20, and (d) CoIr@CN-0.25.

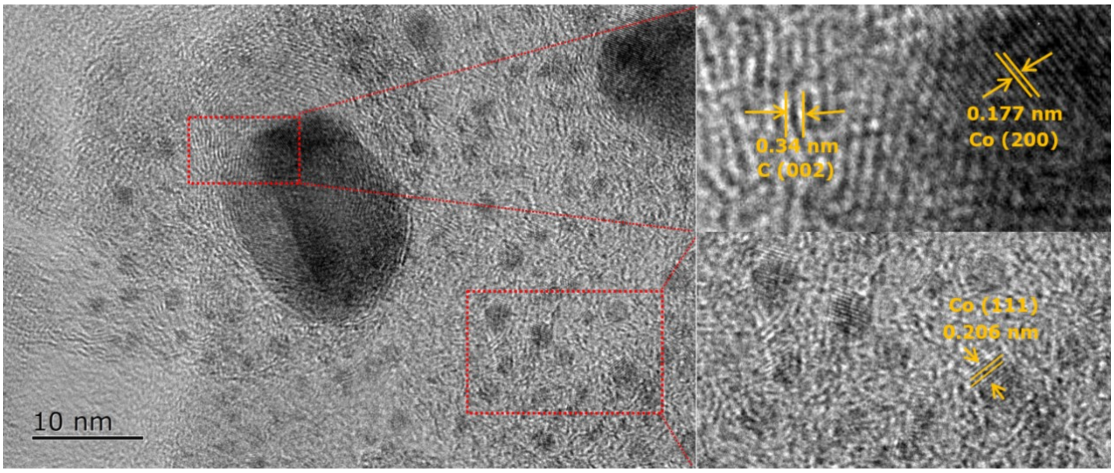

Figure S2. HRTEM images of CoIr@CN-0.20.

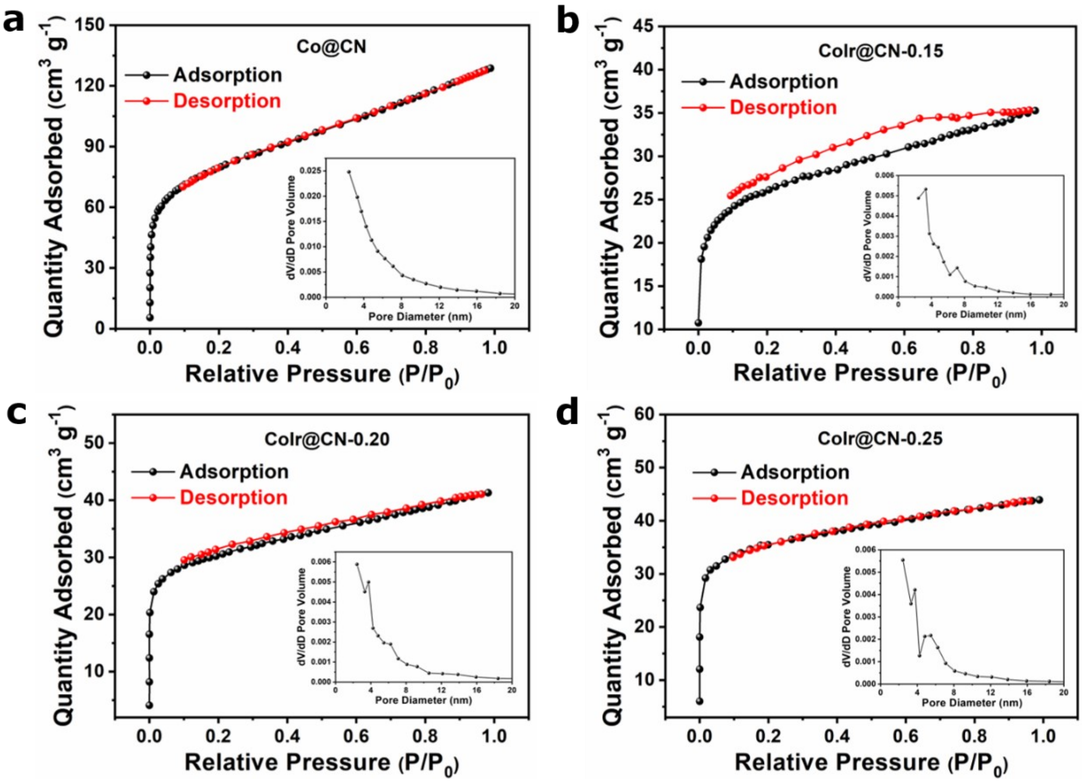

Figure S3. Nitrogen adsorption-desorption isotherms, and (inset) pore size distributions of (a) Co@CN, (b) CoIr@CN-0.15, (c) CoIr@CN-0.20, and (d) CoIr@CN-0.25.

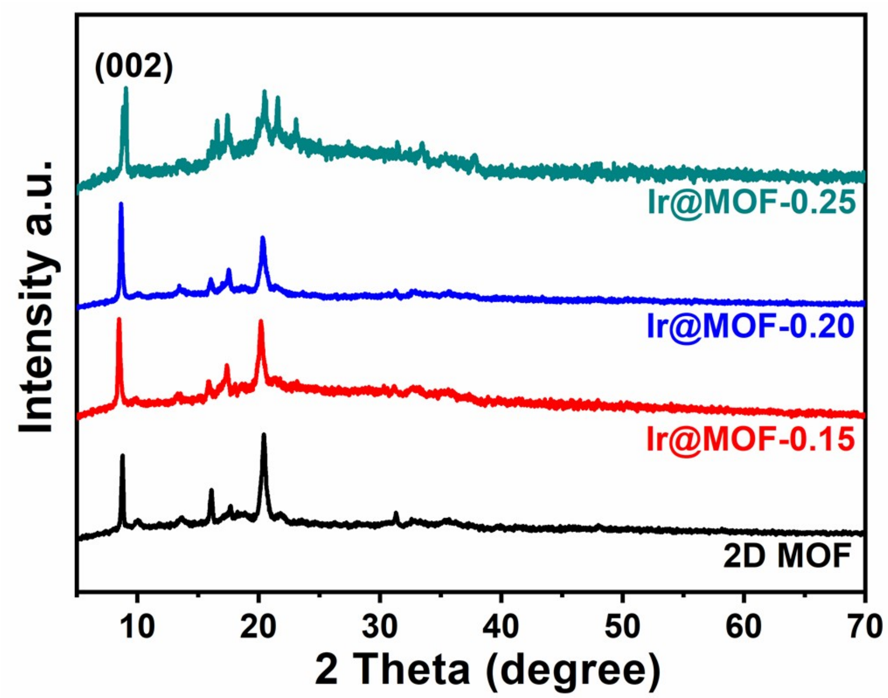

Figure S4. XRD pattern of MOF and Ir@MOF.

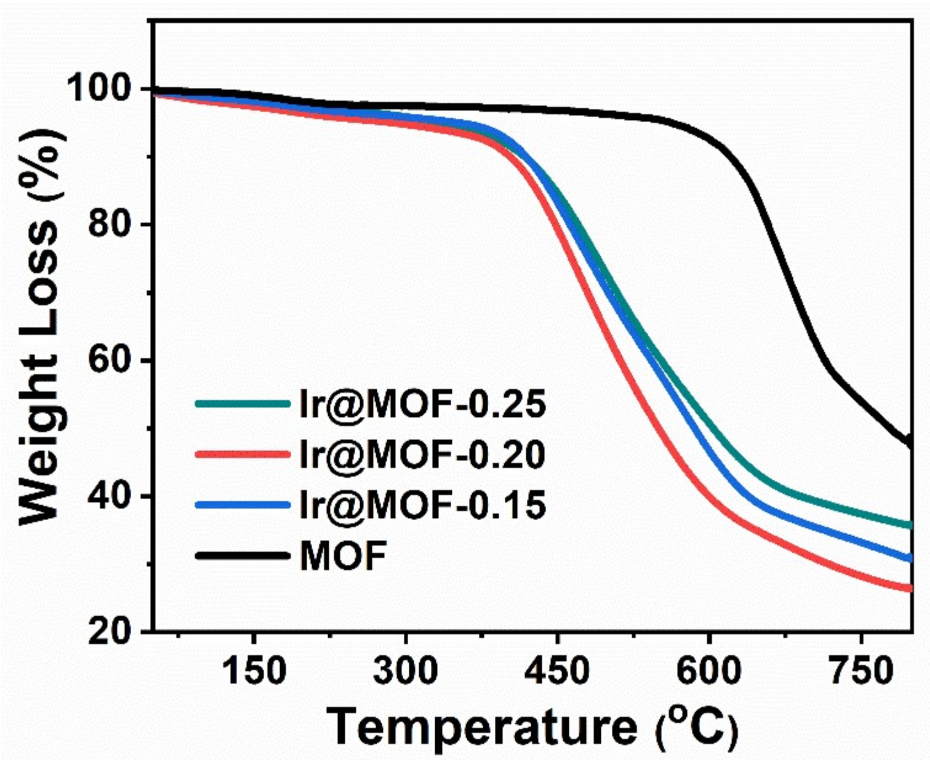

Figure S5. TGA curves of the MOF and Ir@MOF-x (x = 0.15, 0.20, and 0.25) under nitrogen atmosphere.

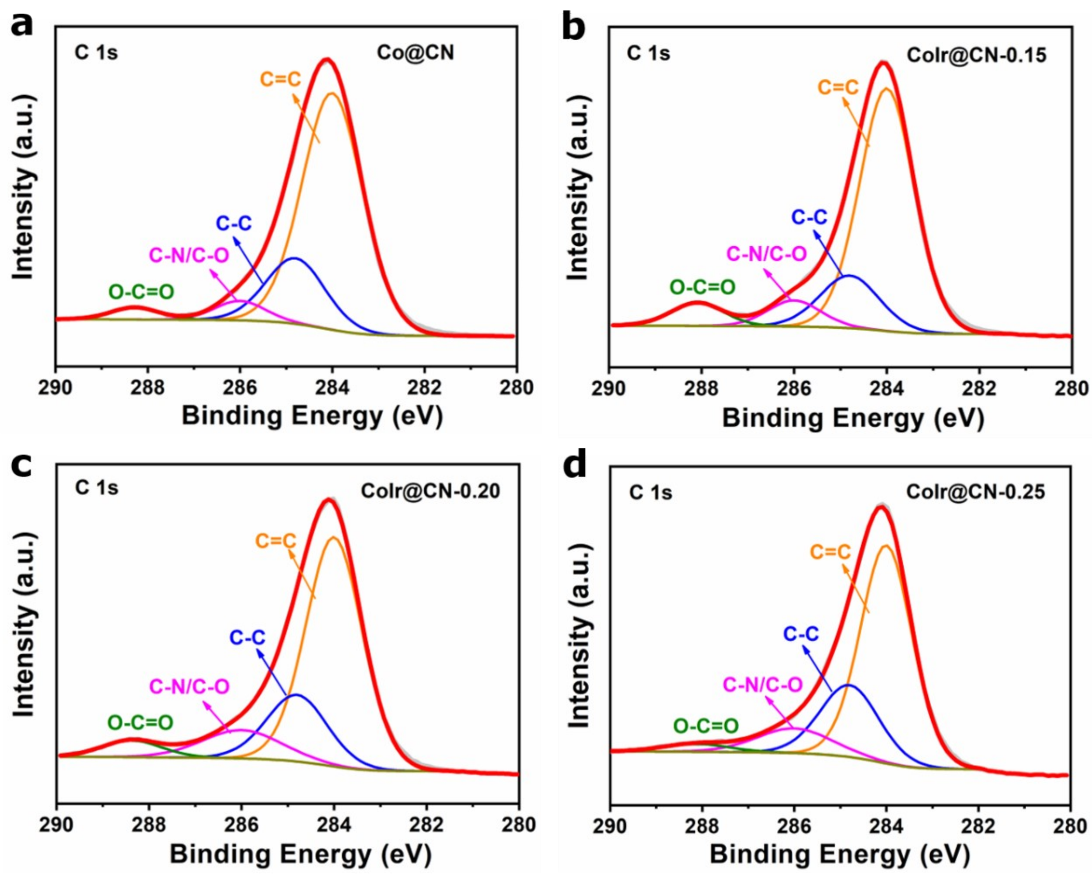

Figure S6. C 1s XPS of (a) Co@CN, (b) CoIr@CN-0.15, (c) CoIr@CN-0.20, and (d) CoIr@CN-0.25.

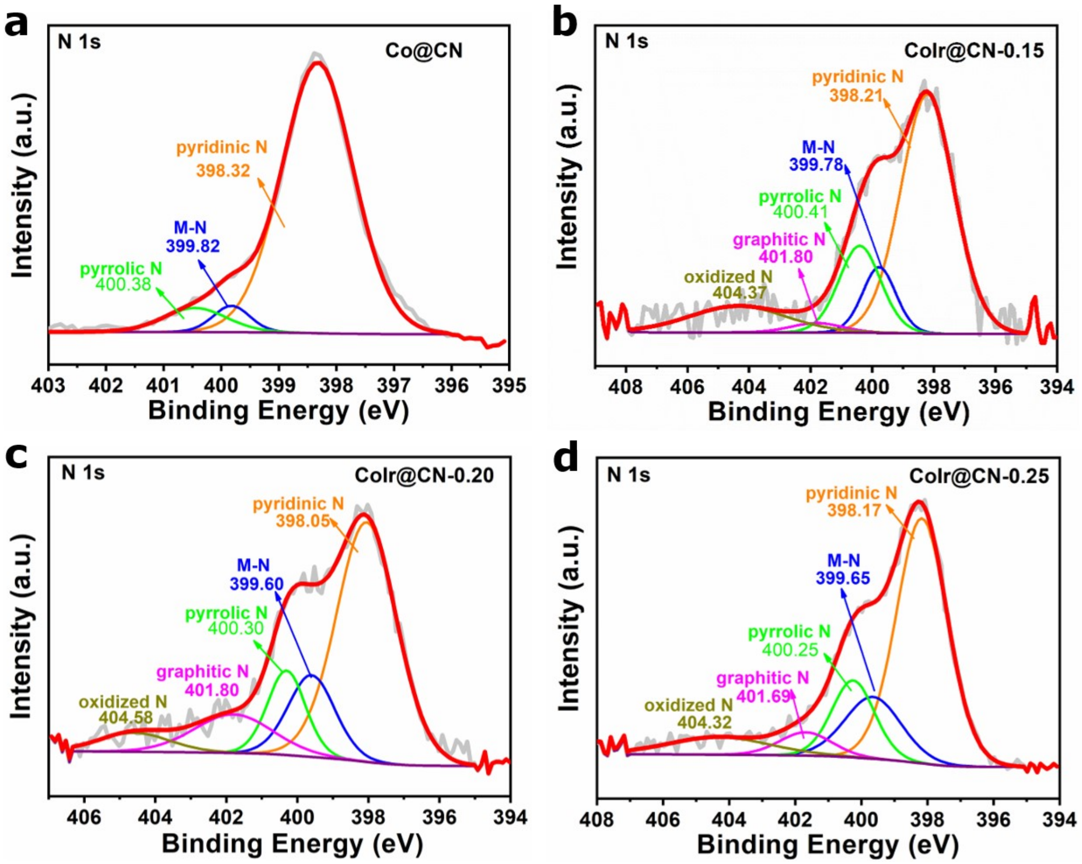

Figure S7. N 1s XPS of (a) Co@CN, (b) CoIr@CN-0.15, (c) CoIr@CN-0.20, and (d) CoIr@CN-0.25.

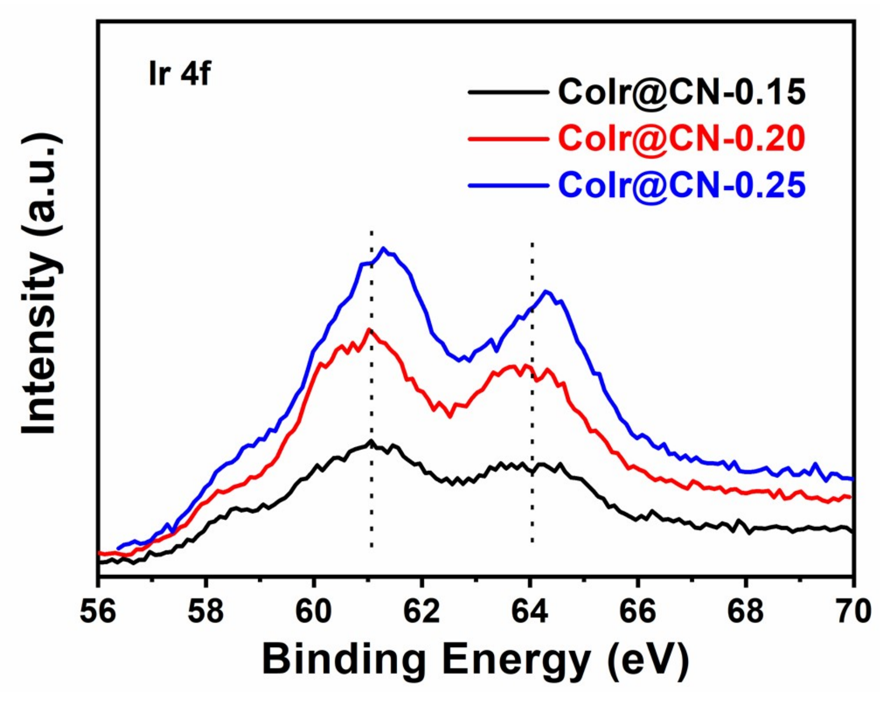

Figure S8. Ir 4f XPS of CoIr@CN-0.15, CoIr@CN-0.20, and CoIr@CN-0.25.

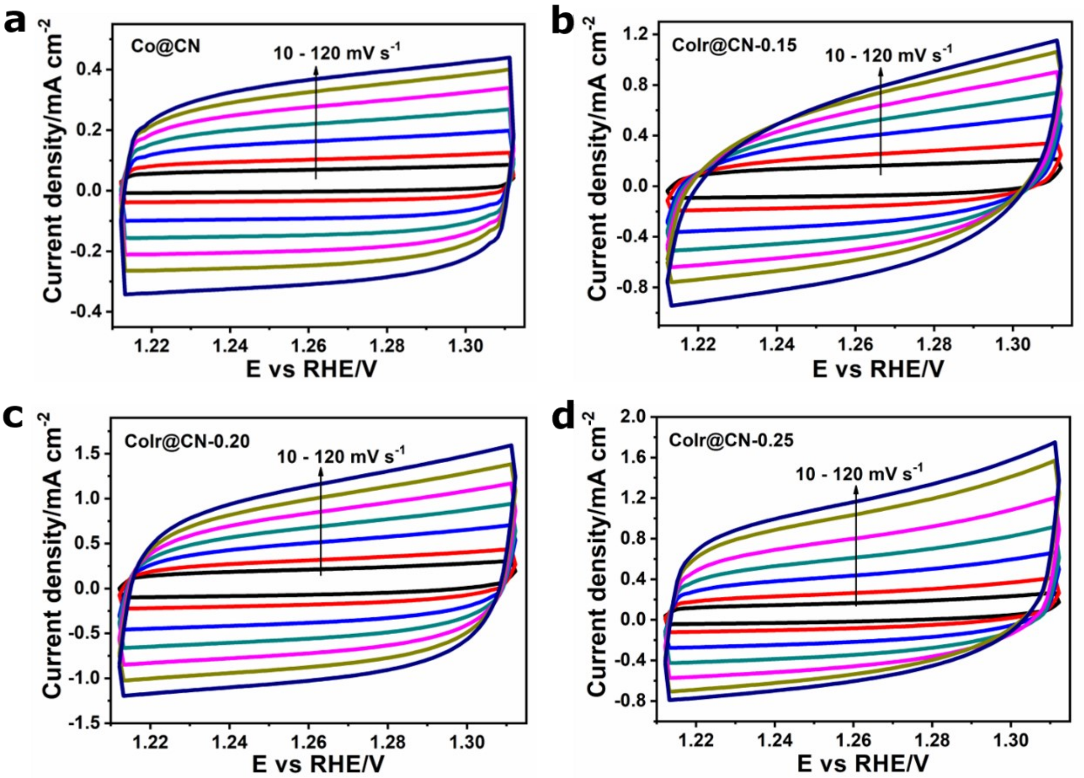

Figure S9. CVs curve of (a) Co@CN, (b) CoIr@CN-0.15, (c) CoIr@CN-0.20, and (d) CoIr@CN-0.25 in 1.0 M KOH for OER.

The corresponding ECSA caculated from C_{dl}:

$$\text{ECSA}_{\text{Co@CN}} = \frac{2.74\ mF\ cm-2}{40\ \mu F\ cm-2} = 68.50\ cm^2$$

$$\text{ECSA}_{\text{CoIr@CN-0.15}} = \frac{5.45\ mF\ cm-2}{40\ \mu F\ cm-2} = 136.25\ cm^2$$

$$\text{ECSA}_{\text{CoIr@CN-0.20}} = \frac{7.37\ mF\ cm-2}{40\ \mu F\ cm-2} = 184.25\ cm^2$$

$$\text{ECSA}_{\text{CoIr@CN-0.20}} = \frac{8.56\ mF\ cm-2}{40\ \mu F\ cm-2} = 214.00\ cm^2$$

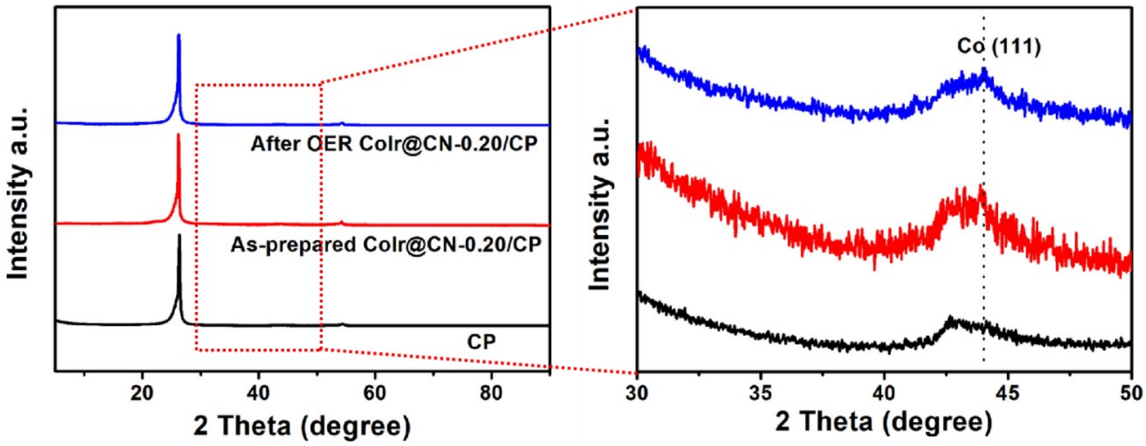

Figure S10. XRD pattern of CoIr@CN-0.20 loaded on carbon paper before and after the long-term OER reaction in 1.0 M KOH.

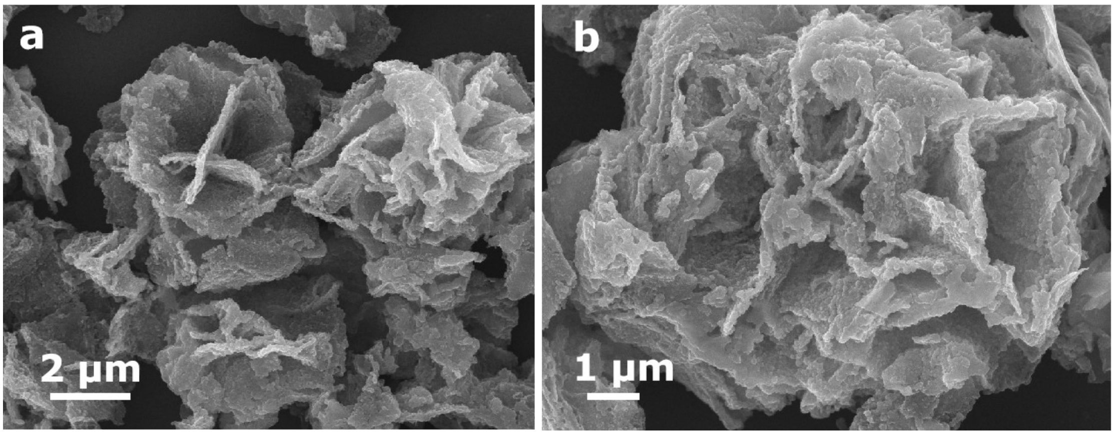

Figure S11. SEM images of CoIr@CN-0.20 after the long-term OER reaction.

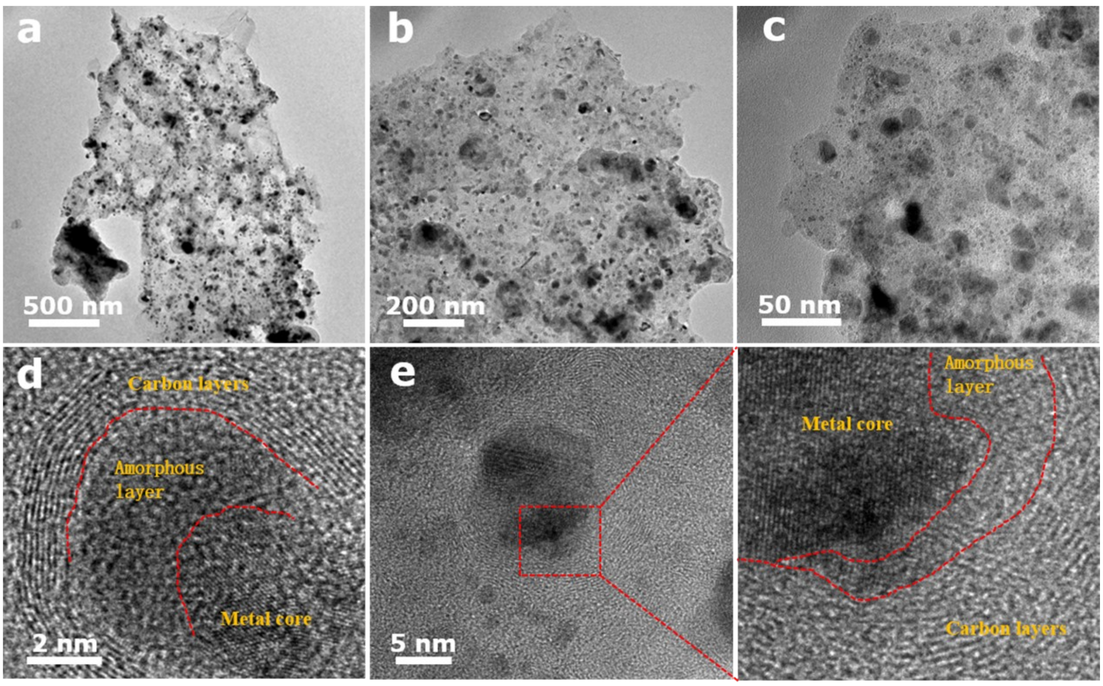

Figure S12. (a-c) Low-magnification TEM and (d, e) High-magnification TEM images of after-OER CoIr@CN-0.20.

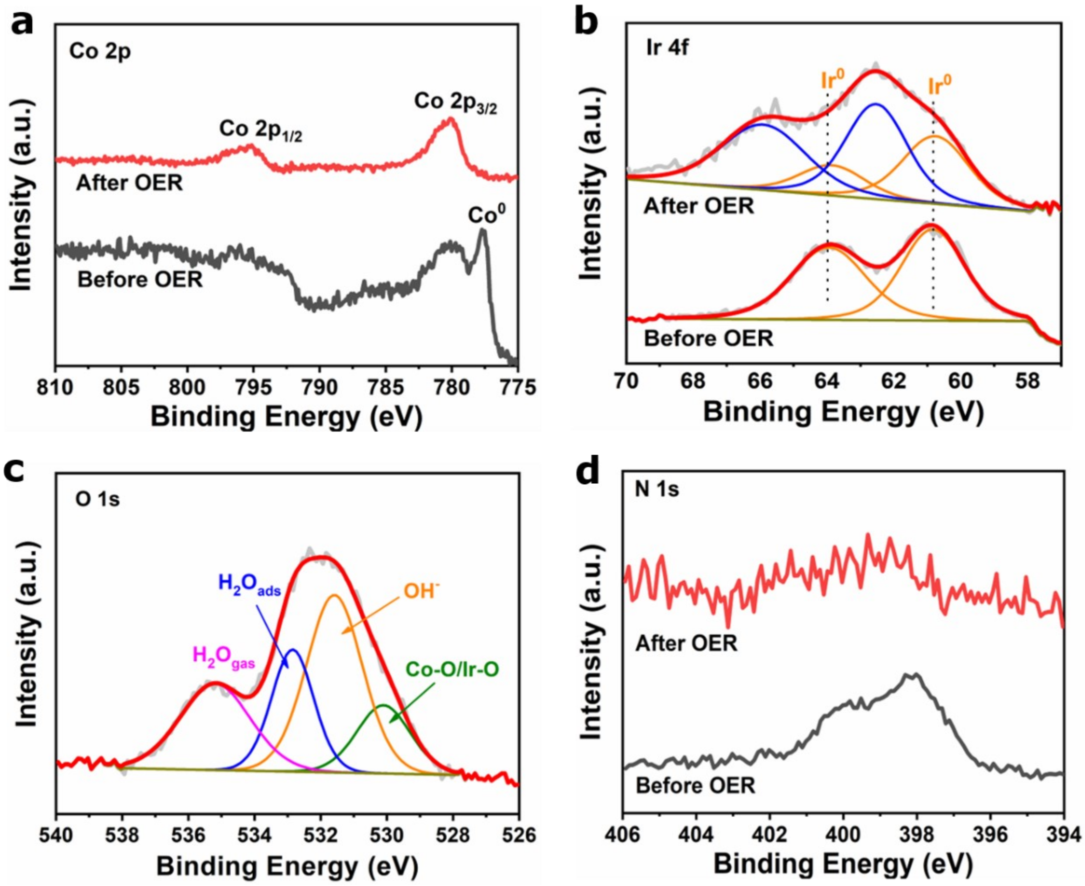

Figure S13. XPS spectra of CoIr@CN-0.20 after long-term OER experiment.

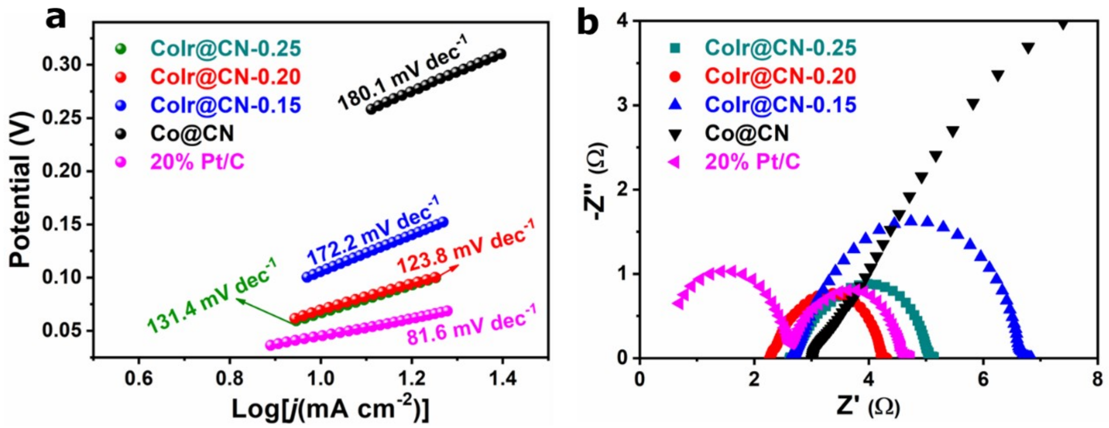

Figure S14. (a) Tafel slope calculated from LSV curves and (b) EIS test in 1.0 M KOH for HER.

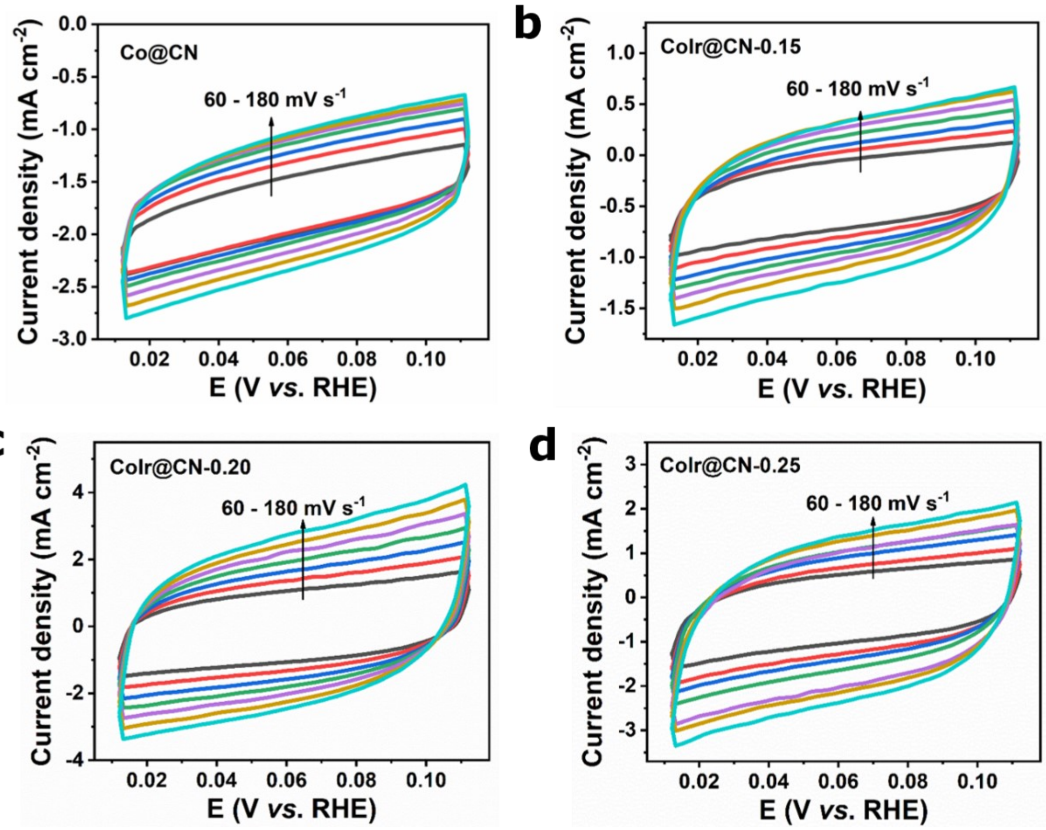

Figure S15. CVs curve of (a) Co@CN, (b) CoIr@CN-0.15, (c) CoIr@CN-0.20, and (d) CoIr@CN-0.25 in 1.0 M KOH for HER.

The corresponding ECSA caculated from C_{dl}:

$$\text{ECSA}_{\text{Co@CN}} = \frac{3.12\ mF\ cm-2}{40\ \mu F\ cm-2} = 78.00\ cm^2$$

$$\text{ECSA}_{\text{CoIr@CN-0.15}} = \frac{3.72\ mF\ cm-2}{40\ \mu F\ cm-2} = 93.00\ cm^2$$

$$\text{ECSA}_{\text{CoIr@CN-0.20}} = \frac{12.75\ mF\ cm-2}{40\ \mu F\ cm-2} = 318.75\ cm^2$$

$$\text{ECSA}_{\text{CoIr@CN-0.25}} = \frac{9.16\ mF\ cm-2}{40\ \mu F\ cm-2} = 229\ cm^2$$

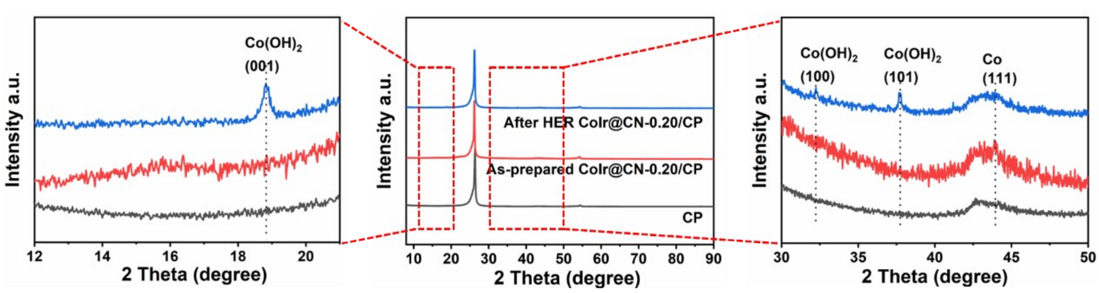

Figure S16. XRD pattern of CoIr@CN-0.20 loaded on carbon paper before and after the long-term HER reaction in 1.0 M KOH.

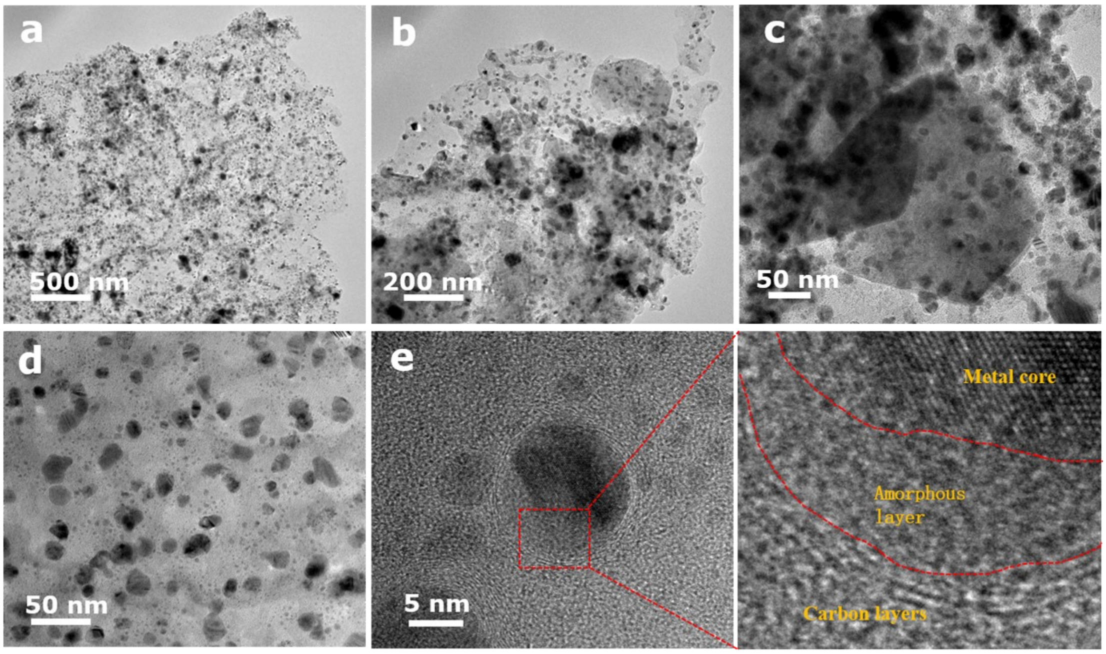

Figure S17. (a-d) Low-magnification TEM and (e) High-magnification TEM images of after-HER CoIr@CN-0.20 in 1.0 M KOH.

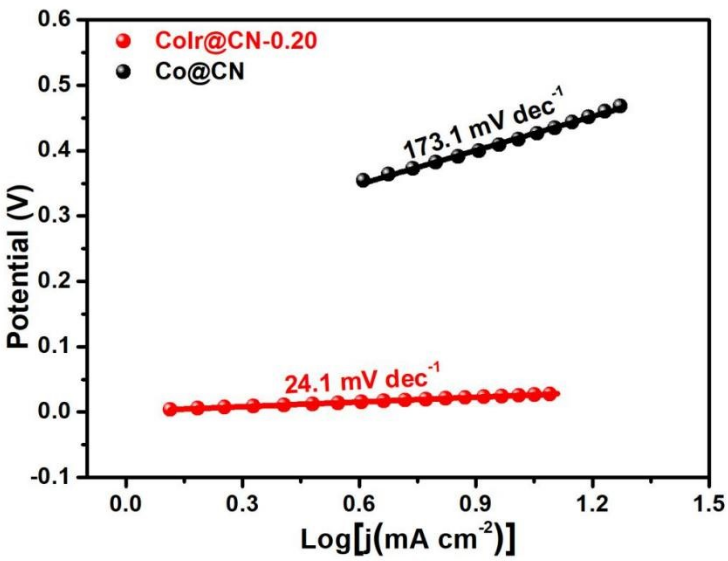

Figure S18. Tafel slope calculated from LSV curves of Co@CN and CoIr@CN-0.20 in 0.5 M H_2SO_4 for HER.

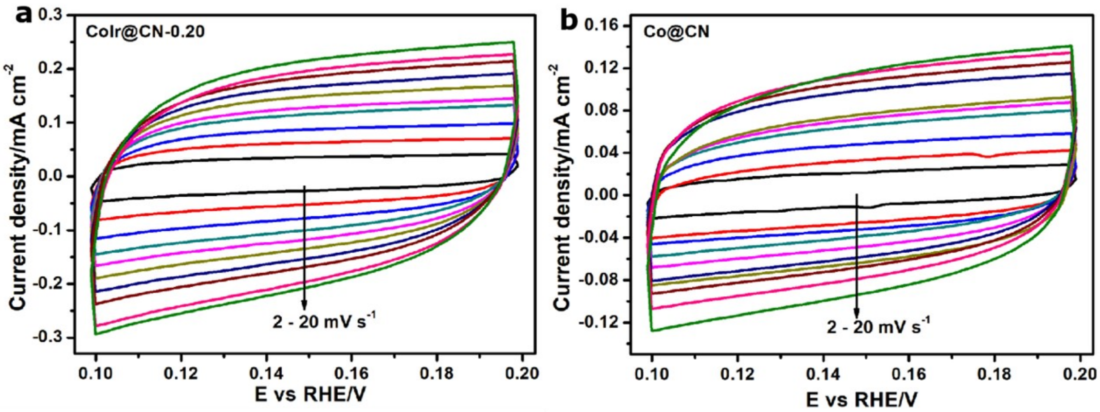

Figure S19. CVs curve of (a) CoIr@CN-0.20 and (b) Co@CN in 0.5 M H_2SO_4 for HER.

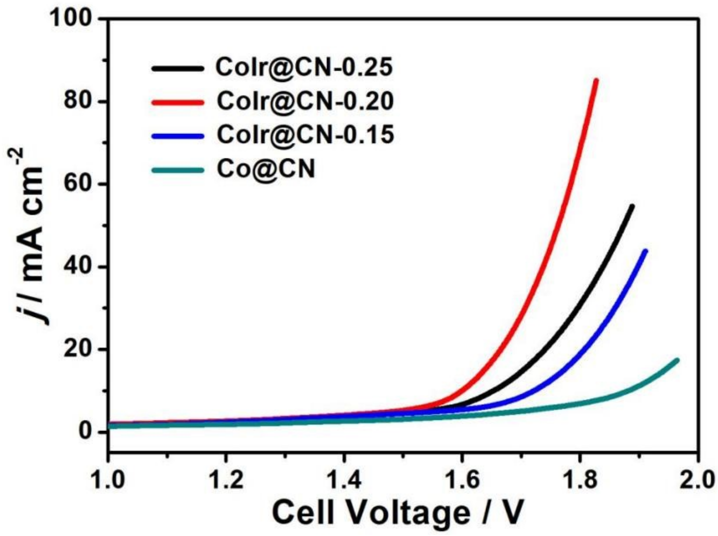

Figure S20. LSV polarization curves of the Co@CN and CoIr@CN-x (x= 0.15, 0.20, 0.25) for water splitting in 1.0 M KOH solution.

Table S1. Loading amount of Co and Ir in Co@CN, CoIr@CN-0.15, CoIr@CN-0.20, and CoIr@CN-0.25 characterized by ICP-MS.

Sample	Co (w%)	Ir (w%)	Molar ratio of Ir and Co
Co@CN	24.57	0	0
CoIr@CN-0.15	47.46	2.55	0.0165
CoIr@CN-0.20	47.31	2.69	0.0175
CoIr@CN-0.25	42.56	2.66	0.0192

Table S2. BET data analysis of Co@CN, CoIr@CN-0.15, CoIr@CN-0.20, and CoIr@CN-0.25 samples.

Sample	Specific Surface Area (m^2 /g)	Pore Volume (cm^3 /g)	Average Pore Size (nm)
Co@CN	276.46	0.1991	2.8801

CoIr@CN-0.15	95.931	0.054529	2.2737
CoIr@CN-0.20	111.95	0.06389	2.2829
CoIr@CN-0.25	128.62	0.067928	2.1125

Table S3. Mass ratios of various elemences in Co@CN, CoIr@CN-0.15, CoIr@CN-0.20, and CoIr@CN-0.25 determined by XPS.

Sample	Co (w%)	Ir (w%)	C (w%)	N (w%)	O (w%)
Co@CN	10.32	-	64.79	10.89	9.69
CoIr@CN-0.15	3.35	6.74	70.77	3.62	15.52
CoIr@CN-0.20	4.69	12.21	64.73	5.34	13.03
CoIr@CN-0.25	4.61	14.35	62.75	5.87	12.43

Table S4. Tafel slope, Exchange current densities (j_o), and Relative j_o of all tested samples for OER.

Samples	Tafel slope (mV dec^{-1})	j_o (mA cm^{-2})	Relative j_o
CoIr@CN-0.25	103.0	0.733	28.19
CoIr@CN-0.20	64.7	0.857	32.96
CoIr@CN-0.15	114.1	0.202	7.77
Co@CN	131.1	0.026	1.0
the commercial RuO_2	164.8	0.025	0.96

Table S5. Tafel slope, Exchange current densities (j_o), and Relative j_o of all tested samples for HER in 1.0 M KOH.

Samples	Tafel slope (mV dec^{-1})	j_o (mA cm^{-2})	Relative j_o
CoIr@CN-0.25	131.4	16.21	29.47
CoIr@CN-0.20	123.8	20.40	37.09
CoIr@CN-0.15	172.2	7.07	12.85
Co@CN	180.1	0.55	1.0
the commercial Pt/C	81.6	33.11	60.2

Table S6. Comparison of OER performance for CoIr@CN-0.20 with other reported carbon-based materials in the 1.0 M KOH.

Catalyst	Electrode	Overpotential at 10 mA cm^{-2} (mV)	Tafel slope (mV dec^{-1})	Reference
CoIr@CN-0.20	CP	269	61.4	This work
Co_3O_4/CN HNPs	GCE	280	59	1
Fe-Co-CN/rGO-700	GCE	308	38	2
hcp-Co@NC	GCE	290	68.2	3
Co-CN hybrids	CP	287	63.8	4
Ir/CN	GCE	265	35	5
CoO_x@CN	GCE	260	-	6
$RuNi_1Co_1$@CMT	CC	299	83	7

Co@Ir/NC-10%	GCE	280	73.8	8
C@NiCo nanospheres	GCE	330	157	9
CoP(MoP)-$CoMoO_3$@CN	GCE	296	105	10
Co@N-CNTF	GCE	350	61.4	13

Table S7. Comparison of HER performance for CoIr@CN-0.20 with other reported carbon-based materials in the 1 M KOH or 0.5 M H_2SO_4.

Catalyst	Electrode	Electrolyte	Potential at 10 mA cm^{-2} (mV)	Tafel slope (mV dec^{-1})	Reference
CoIr@CN-0.20	CP	1 M KOH	70	123.8	This work
CoIr@CN-0.20	CP	0.5 M H_2SO_4	25	24.1	This work
Fe-Co-CN/rGO-700	GCE	1 M KOH	215	54	2
hcp-Co@NC	GCE	1 M KOH	90	90.7	3
$RuNi_1Co_1$@CMT	carbon cloth	1 M KOH	78	77	7
Co@Ir/NC-10%	GCE	1 M KOH	121	38	8
C@NiCo nanospheres	GCE	1 M KOH	105	106	9
CoP(MoP)-$CoMoO_3$@CN	GCE	1 M KOH	198	95	10
G@Co-W-P	GCE	1 M KOH	102.3	61.2	11
G@Co-W-P	GCE	0.5 M H_2SO_4	91.5	40.7	11
IrCo@NC-500	GCE	1 M KOH	45	80	12
IrCo@NC-500	GCE	0.5 M H_2SO_4	24	23	12
Co@N-CNTF	GCE	1 M KOH	226	-	13
Co@N-CNTF	GCE	0.5 M H_2SO_4	220	-	13

References

[1] X. Chen, Y. Chen, X. Luo, H. Guo, N. Wang, D. Su, C. Zhang, T. Liu, G. Wang, L. Cui, *Appl. Surf. Sci.*, 2020, **526**, 14662.

[2] W. Fang, J. Wang, Y. Hu, X. Cui, R. Zhu, Y. Zhang, C. Yue, J. Dang, W. Cui, H. Zhao, Z. Li, *Electrochim. Acta,* 2021, **365**, 137384.

[3] N. Li, H. Tan, X. Ding, H. Duan, W. Hu, G. Li, Q. Ji, Y. Lu, Y. Wang, F. Hu, C. Wang, W. Cheng, Z. Sun, W. Yan, *Appl. Catal. B-Environ.,* 2020, **266**, 118621.

[4] X. Wang, M. Liu, H. Zhang, S. Yan, C. Zhang, S. Liu, *Nano Res.,* 2021, **14**, 4569-4576.

[5] H. Wang, M. Ming, M. Hu, C. Xu, Y. Wang, Y. Zhang, D. Gao, J. Bi, G. Fan, J.S. Hu, *ACS Appl. Mater. Interfaces*, 2018, **10**, 22340-22347.

[6] H. Jin, J. Wang, D. Su, Z. Wei, Z. Pang, Y. Wang, *J. Am. Chem. Soc,* 2015, **137**, 2688.

[7] Y. Xue, Q. Yan, X. Bai, Y. Xu, X. Zhang, Y. Li, K. Zhu, K. Ye, J. Yan, D. Cao, G. Wang, *J. Colloid Interface Sci.*, 2022, **612**, 710.

[8] D. Li, Z. Zong, Z. Tang, Z. Liu, S. Chen, Y. Tian, X. Wang, *ACS Sustainable Chem. Eng.,* 2018, **6**, 5105-5114.

[9] S. Tan, W. Ouyang, Y. Ji, Q. Hong, *J. Alloy. Compd.,* 2021, **889**, 161528.

[10] L. Yu, Y. Xiao, C. Luan, J. Yang, H. Qiao, Y. Wang, X. Zhang, X. Dai, Y. Yang, H. Zhao, *ACS Appl. Mater. Interfaces*, 2019, **11**, 6890-6899.

[11] X. Wang, J.B. Le, Y. Fei, R. Gao, M. Jing, W. Yuan, C.M. Li, *J. Mater. Chem. A*, 2022, **10**, 7694-7704.

[12] P. Jiang, J. Chen, C. Wang, K. Yang, S. Gong, S. Liu, Z. Lin, M. Li, G. Xia, Y. Yang, J. Su, Q. Chen, *Adv. Mater.,* 2018, **30**, 1705324.

[13] H. Guo, Q. Feng, J. Zhu, J. Xu, Q. Li, S. Liu, K. Xu, C. Zhang, T. Liu, *J. Mater. Chem. A*, 2019, 7, 3664-3672.